Oxidation of [2Fe–2S] Isoferredoxins with $[Co(NH_3)_6]^{3+}$ and $[Cr(phen)_3]^{3+}$ (phen = 1,10-phenanthroline): Mechanism of Electron Transfer†

Emma Lloyd, Nicholas P. Tomkinson and A. Geoffrey Sykes*
Department of Chemistry, The University, Newcastle upon Tyne NE1 7RU, UK

The reactivity of different isoferredoxins, FdI and FdII, has been investigated for the first time. Similar saturation kinetic behaviour is observed in the oxidation of FdI and FdII, from spinach, parsley and *Anabaena variabilis*, with $[Co(NH_3)_6]^{3+}$, highlighting the importance of conserved residues. Studies with the oxidant $[Cr(phen)_3]^{3+}$ (phen = 1,10-phenanthroline) have also been made for the first time. Both proteins are blocked by redox-inactive $[Cr(NH_3)_6]^{3+}$ (K_B = 525 for spinach FdII and 512 M^{-1} for parsley FdI), in agreement with previously determined values of ≈470 M^{-1}. Use of the same site on the protein surface, influenced by favourable electrostatic interactions, but independent of ligand type on the complex (NH_3 or phen), is indicated. A site for reaction incorporating surface aromatic residues Tyr25/Tyr82, an acidic path, and a surface contour (hollow) region is implicated on the basis of kinetic and previous NMR studies. Factors affecting electron transfer to the oxidant at this site are considered.

The [2Fe–2S] ferredoxins (M_r ≈ 10 500, 93–99 amino acids) from higher plants and algae are involved in biological electron transfer, $Fe^{III}_2 + e^- \rightleftharpoons Fe^{II}Fe^{III}$ ($E^\circ \approx -400$ mV). It is now known that isolation procedures yield a mixture of two isoferredoxins.[1] These can be separated using hydrophobic interaction columns,[2] and are generally referred to as FdI and FdII in order of elution. The reasons for the existence of two forms is not clear. In the case of spinach the relative amounts of FdI and FdII are close to 75:25.[2] The sequences have been determined and 25 amino acids were found to be different. Similarly other ferredoxins have been shown to have two components,[2,3] which raises questions concerning earlier kinetic studies on FdI and FdII mixes from spinach,[4] parsley,[4,5] and *Spirulina plastensis*,[6] and whether interpretations given at that time are correct. Some checks are appropriate, and these have now been carried out in the most economic way possible with $[Co(NH_3)_6]^{3+}$ as oxidant for protein in the $Fe^{II}Fe^{III}$ state, equation (1).

$$Fe^{II}Fe^{III} + Co^{III} \longrightarrow Fe^{III}_2 + Co^{II} \quad (1)$$

Ferredoxins from three sources, spinach, parsley and *Anabaena variabilis*, were tested. The structure of *A. variabilis* FdI has been reported recently.[7] The overall structure is similar to that of *Spirulina platensis* and *Aphanothece sacrum* [2Fe–2S] ferredoxins,[8,9] but some differences have been noted.[7] At the same time, so that we can comment further on the nature of the reactions and the relative importance of electrostatics as opposed to hydrogen-bonding and/or stacking of aromatic residues, we have studied the reactions of just two of these ferredoxins, spinach FdII and parsley FdI, with $[Cr(phen)_3]^{3+}$ (phen = 1,10-phenanthroline) as oxidant (−260 mV).

Experimental

Protein Sources.—Procedures for the isolation of ferredoxin from spinach[4,10] and parsley[4,11] leaves have been reported. *Anabaena variabilis* blue-green algae were grown in 10–20 l vessels,[12,13] and the ferredoxin isolated as previously described.[14] Samples were stored at −20 °C under N_2. Protein purity was checked using ratios of absorbance at 422 and 278 nm. Ratios of $A_{422}/A_{278} > 0.46:1$ (0.50:1 here) for spinach FdI and FdII, of >0.60:1 (0.62:1 here) for parsley FdI and FdII, and >0.60:1 (0.62:1 here) for *A. variabilis* were considered satisfactory.

Separation of FdI *and* FdII *Components.*—The procedure employed was an adaptation of that used by Sakihama *et al.*[2] A Phenyl Superose HR 5/5 hydrophobic interaction column attached to a Pharmacia FPLC system was used. Elution was monitored at 280 nm using a UV-M control. All buffers were degassed with N_2 before use to minimise loss of ferredoxin. The running buffers were: A, 20 mM Tris–HCl at pH 7.5; B, 20 mM Tris–HCl containing 1.7 M ammonium sulfate at pH 7.5 [Tris = tris(hydroxymethyl)aminomethane]. The column was equilibrated in buffer B and the ferredoxin sample loaded in the same buffer. Separation was achieved using a linear gradient (1.75% per cm^3) of 0–50% A with a flow rate of 0.5 cm^3 min^{-1}. The ferredoxins separated into major (FdI) and minor (FdII) components in a ratio of 77% FdI to 23% FdII (spinach), 74 to 26% (parsley), and 91 to 9% (*A. variabilis*).

Complexes.—A sample of hexaaminecobalt(III) chloride, $[Co(NH_3)_6]Cl_3$, was prepared as in previous studies[4] [UV/VIS absorbance spectra peak positions λ/nm (ε/M^{-1} cm^{-1}) 339 (46.4) and 473 (57.1)].[15] The tris(1,10-phenanthroline)chromium(III) complex, $[Cr(phen)_3]Cl_3 \cdot 6H_2O$ [λ/nm 430(sh), 320(sh) and 276 (ε = 3.98 × 10^4 M^{-1} cm^{-1})] was also prepared with HCl substituted for $HClO_4$ in the procedure.[16] The reduction potential of the $[Co(NH_3)_6]^{3+/2+}$ couple is estimated as ≈ 100 mV,[17] and that of $[Cr(phen)_3]^{3+/2+}$ is −260 mV.[16] Redox-inactive $[Cr(NH_3)_6]Cl_3 \cdot H_2O$ was prepared as previously.[5] Peat positions λ/nm (ε/$M^{-1}cm^{-1}$) were in good agreement (±0.2%) with the previous values 350 (33) and 462 (40).

Kinetic Studies.—Reactions were monitored at 422 nm (Δε 4900 M^{-1} cm^{-1}) on a Dionex-D110 stopped-flow spectrophotometer. Stoichiometric equations as in (1) have been established,[4] and are assumed to apply here also. Rate constants (25 °C) were obtained using fitting procedures and programs from On-Line Instrument Systems (OLIS, Jefferson, GA, USA). Rate con-

† *Non-SI units employed:* M = mol dm^{-3}.

Table 1 First-order rate constants (k_{obs}) for the 1:1 oxidation of different [2Fe–2S] ferredoxins with (*a*) $[Co(NH_3)_6]^{3+}$ and (*b*) $[Cr(phen)_3]^{3+}$ at 25 °C, pH 8.0 (Tris–HCl), I = 0.100 M (NaCl)

Spinach FdI (3.0×10^{-5} M)	
$[Co(NH_3)_6^{3+}]$ mM	0.24, 0.49, 0.99, 1.98, 3.93, 4.87
k_{obs}/s^{-1}	3.12, 4.55, 7.28, 9.69, 11.8, 12.7
Spinach FdII (3.6×10^{-5} M)	
$[Co(NH_3)_6^{3+}]$/mM	0.24, 0.49, 0.99, 1.98, 3.93, 4.87
k_{obs}/s^{-1}	4.87, 7.33, 10.4, 14.6, 16.5, 17.4
Parsley FdI (3.6×10^{-5} M)	
$[Co(NH_3)_6^{3+}]$/mM	0.26, 0.51, 0.98, 1.98, 3.96, 4.92
k_{obs}/s^{-1}	4.31, 6.6, 8.9, 12.1, 15.4, 16.3
A. variabilis FdI (4.1×10^{-5} M)	
$[Co(NH_3)_6^{3+}]$/mM	0.26, 0.51, 0.98, 1.98, 3.96, 4.92
k_{obs}/s^{-1}	1.11, 1.75, 2.25, 2.96, 4.0, 4.2
Spinach FdII (3.6×10^{-5} M)	
$[Cr(phen)_3]^{3+}$/mM	0.25, 0.50, 1.00, 2.00, 4.00, 5.00
k_{obs}/s^{-1}	2.45, 4.42, 7.1, 9.8, 12.2, 13.3
Parsley FdI (3.6×10^{-5} M)	
$[Cr(phen)_3]^{3+}$/mM	0.25, 0.50, 1.00, 2.00, 4.00, 5.00
k_{obs}/s^{-1}	2.4, 4.2, 5.8, 8.6, 11.2, 12.0

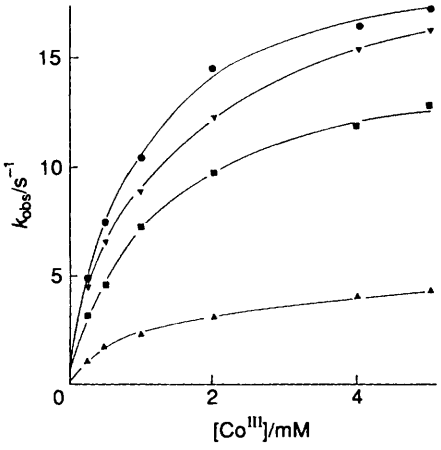

Fig. 1 Variation of rate constants (25 °C) with concentration of oxidant $[Co(NH_3)_6]^{3+}$ (reactant in excess), for different [2Fe–2S] ferredoxins: spinach FdI (■), spinach FdII (●), parsley FdI (▼) and *A. variabilis* FdI (▲), at pH 8.0 (Tris–HCl), I = 0.100 M (NaCl)

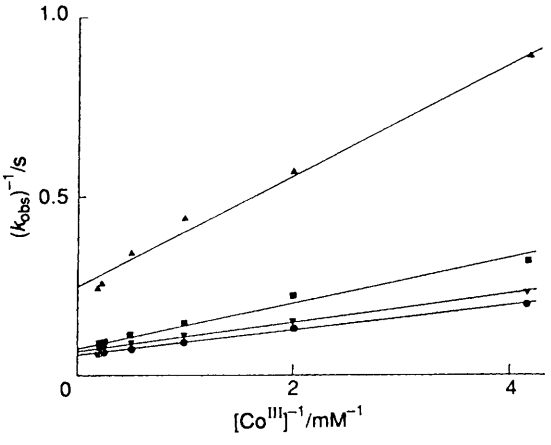

Fig. 2 Dependence of rate constants (25 C) on oxidant $[Co(NH_3)_6^{3+}]$ (reactant in excess) for reaction with different [2Fe 2S] ferredoxins. Details as in Fig. 1

stants reported were an average of at least five-stopped-flow traces for the same reactant solutions. The buffer used was 20 mM Tris–HCl at pH 8.0, and the ionic strength was adjusted to I = 0.100 M (NaCl). Protein reactant solutions were obtained by reduction with sodium dithionite as described previously.[4-6]

Table 2 Summary of association constants (K) and electron-transfer rate constants (k_{et}) for the 1:1 oxidation of different [2Fe–2S] ferredoxins with (*a*) $[Co(NH_3)_6]^{3+}$ and (*b*) $[Cr(phen)_3]^{3+}$ at 25 °C, pH 8.0 (Tris–HCl), I = 0.100 M (NaCl). Standard deviations are shown in parentheses

Protein	K/M^{-1}	k_{et}/s^{-1}
(*a*) $[Co(NH_3)_6]^{3+}$ as oxidant		
Spinach FdI	914(68)	15.2(0.4)
Spinach FdII	1156(96)	20.0(0.5)
Spinach (mix)[a]	933	15.9
Parsley FdI	917(97)	19.5(0.7)
Parsley (mix)[a]	988	19.2
A. variabilis FdI	938(115)	5.1(0.2)
S. platensis (mix)[b]	2070	4.9
(*b*) $[Cr(phen)_3]^{3+}$ as oxidant		
Spinach FdII	733(53)	16.5(0.4)
Parsley FdI	670(68)	15.3(0.6)

[a] Ref. 4. [b] Ref. 6.

Table 3 Rate constants (25 °C) for the $[Cr(NH_3)_6]^{3+}$ inhibition of the $[Cr(phen)_3]^{3+}$ (3.0×10^{-4} M) oxidation of (*a*) spinach FdII and (*b*) parsley FdI, both 2.9×10^{-5} M, I = 0.100 M (NaCl)

(*a*)	$[Cr(NH_3)_6^{3+}]$/M	0.25, 0.50, 1.0, 2.0, 4.0
	k_{obs}/s^{-1}	2.90, 2.84, 2.09, 1.47, 0.95
(*b*)	$[Cr(NH_3)_6^{3+}]$/M	0.25, 0.50, 1.0, 2.0, 4.0
	k_{obs}/s^{-1}	2.77, 2.34, 1.95, 1.45, 0.90

Results

$[Co(NH_3)_6]^{3+}$ *as Oxidant*.—Kinetic studies were with $[Co(NH_3)_6]^{3+}$ in large >10-fold excess of the [2Fe–2S] protein. First-order rate constants (k_{obs}) obtained by monitoring the $Fe^{II}Fe^{III} \longrightarrow Fe^{III}_2$ change for four different FdI and FdII components are listed in Table 1. These give non-linear dependences on $[Co(NH_3)_6^{3+}]$, Fig. 1, consistent with equations (2) and (3), in which the rapid association (K)

$$Fe^{II}Fe^{III} + Co^{III} \overset{K}{\rightleftharpoons} Fe^{II}Fe^{III}, Co^{III} \quad (2)$$

$$Fe^{II}Fe^{III}, Co^{III} \xrightarrow{k_{et}} Fe^{III}_2 + Co^{II} \quad (3)$$

precedes electron-transfer (k_{et}). From equations (2) and (3) expression (4) is derived, and the data is seen to conform to

$$k_{obs} = \frac{Kk_{et}[Co^{III}]}{1 + K[Co^{III}]} \quad (4)$$

this rate law by plotting $(k_{obs})^{-1}$ against $[Co^{III}]^{-1}$, Fig. 2. Values of K and k_{et} were obtained from an unweighted non-linear least-squares program, and are as listed in Table 2.

$[Cr(phen)_3]^{3+}$ *as Oxidant*.—Rate constants for spinach FdII and parsley FdI were determined, Table 1. The treatment of data was as above. Values of K and k_{et} are listed in Table 2. Competitive inhibition is observed using redox-inactive $[Cr(NH_3)_6]^{3+}$, Table 3, and is of the form described in earlier work,[5] in the course of which an average value of K_B = 468 M^{-1} was obtained for parsley [2Fe–2S]. The dependence is described by equation (5). In the present studies with spinach

$$\frac{k_{obs}}{[Cr(phen)_3^{3+}]} = \frac{Kk_{et}}{1 + K_B[Cr(NH_3)_6^{3+}]} \quad (5)$$

FdII, K_B = 525 ± 36 M^{-1} and with parsley FdI, K_B = 512 ± 34 M^{-1}.

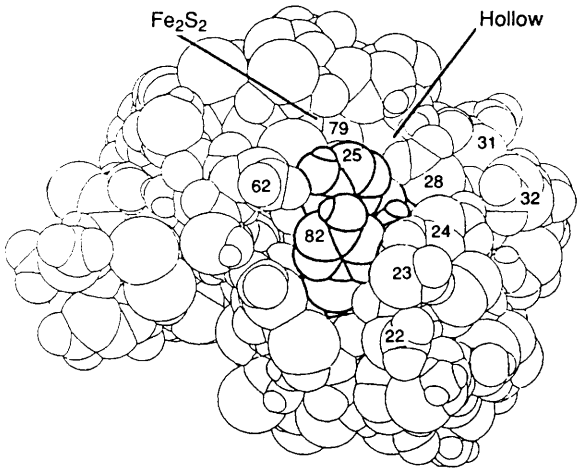

Fig. 3 Part of the surface of [2Fe–2S] ferredoxin as determined by X-ray crystallography for the protein from *A. variabilis*.[7] The space-filling display shown was obtained on a Silicon Graphics screen using the program QUANTA. The numbers refer to amino-acid residues in the polypeptide chain. The aromatic rings of Tyr25 and Tyr82 are indicated in bold

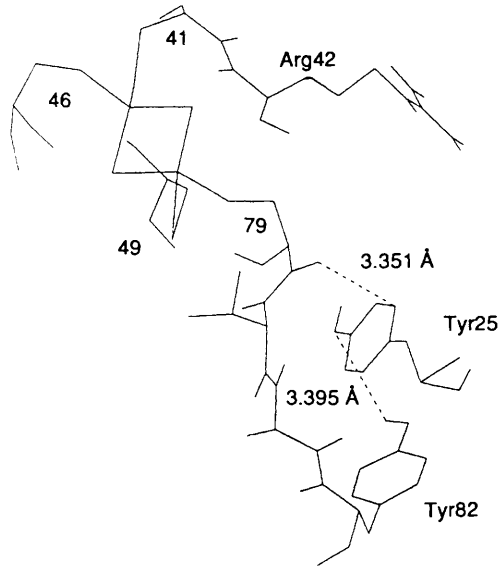

Fig. 4 An assessment of possible routes for electron transfer in [2Fe–2S] ferredoxins from X-ray crystallographic information for the protein from *A. variabilis*. The active-site cysteine ligands 41, 46, 49 and 79, arginine 42 and the aromatic rings of tyrosines 25 and 82 are indicated

Discussion

The reactions of ferredoxin FdI and FdII forms from spinach, parsley and *A. variabilis* have been studied with two oxidants, $[Co(NH_3)_6]^{3+}$ and $[Cr(phen)_3]^{3+}$. In all cases, saturation kinetics are observed. The results obtained with $[Co(NH_3)_6]^{3+}$ as oxidant show little variation in K (914–1160 M^{-1}) for association prior to electron transfer k_{et} (5.1–20 s^{-1}). For the reaction of $[Cr(phen)_3]^{3+}$ with reduced ferredoxin the aim was to assess whether differences in the ligand type on the oxidant have any effect on the reaction and hence help to identify the probable reaction site. Two different ferredoxins, parsley FdI and spinach FdII, were tested. Different ferredoxins from the same source did not need to be checked since consistency between the two forms with $[Co(NH_3)_6]^{3+}$ as oxidant had already been established. The parameters obtained for the two $[Cr(phen)_3]^{3+}$ reactions, K (670–733 M^{-1}) and k_{et} (15.3–16.5 s^{-1}), show close similarity to those for $[Co(NH_3)_6]^{3+}$. No major differences in reactivity are apparent for these different ferredoxin components. Both oxidants are inhibited by redox-inactive $[Cr(NH_3)_6]^{3+}$ with the same K_B value, and reaction at the same site (or sites) on the protein surface is implicated. Differences in the type of ligand on the oxidant do not appear to be relevant therefore. Thus, in terms of K values there is no obvious advantage in using $[Co(NH_3)_6]^{3+}$, which could conceivably hydrogen-bond to the protein, compared to $[Cr(phen)_3]^{3+}$ which has ligands able to interact with aromatic residues (no hydrogen bonding). Furthermore, the kinetics are only marginally affected by differences between FdI and FdII components and electrostatics appear to be the prime controlling feature.

Values for the association constant K of $\approx 10^3$ M^{-1} for $[Co(NH_3)_6]^{3+}$, $[Cr(phen)_3]^{3+}$ and $[Cr(NH_3)_6]^{3+}$ combined with values for a range of other cationic inorganic complexes[4–6] are consistent with interactions at a negatively charged site on the protein. A conserved site is required therefore which is not influenced by differences in the cationic complexes used here, and can interact with all of them in the same manner. An analysis of the amino-acid composition[3] of these ferredoxins reveals an overwhelming array of negatively charged residues, and overall estimates of charge on the reduced protein are 17 – for spinach FdI, 16 – for spinach FdII, 18 – for parsley FdI and *A. variabilis* FdI, and 19 – for *S. platensis*. Despite the unusually high net negative charges on the proteins, there is no evidence for a greater than first-order dependence on oxidant concentration.

Extensive NMR studies which complement the above kinetic findings have been carried out by Markley and co-workers,[18] using $[Cr(NH_3)_6]^{3+}$ as a paramagnetic probe in an attempt to rationalise further the exact location of the binding site. In the presence of a 1:30 molar ratio of $[Cr(NH_3)_6]^{3+}$ to protein, selective broadening of the resonances assigned to Tyr82 in *A. variabilis* ferredoxin is observed (numbering as in the crystal structure).[7] The complex $[Cr(CN)_6]^{3-}$ has no similar effect, even at concentrations >1:5 molar equivalents and it was concluded that $[Cr(NH_3)_6]^{3+}$ binds close to the aromatic rings of Tyr25 and 82. In addition the oxidoreductase and $[Cr(NH_3)_6]^{3+}$ bind competitively at the same site. Combined with the kinetic data, these results are particularly illuminating and the evidence is consistent with a single recognition site that is used by $[Co(NH_3)_6]^{3+}$, $[Cr(phen)_3]^{3+}$ and ferredoxin–$NADP^+$ (nicotinamide–adenine dinucleotide phosphate) oxidoreductase as well as redox-inactive $[Cr(NH_3)_6]^{3+}$.

An attractive feature of a binding site at or near to Tyr82 and 25 is the number of conserved negatively charged residues in close proximity. Attention has been drawn to the importance of Asp22, 23 and 62 (Asp63 in ref. 18), and there are others, namely the conserved acidic residues at position 28, 31 and 32 in the same locality, Fig. 3. Paramagnetic broadening of the resonances of an additional residue Glu24 present in *A. variabilis* FdI were observed,[18] and the latter is also implicated in the binding site. This region of surface has therefore all the requisites for a functionally important site.

Tsukihara *et al.*[9] have suggested the hollow contour of negative electrostatic potential located between Tyr25 and the active site as the binding site, Fig. 3. It was suggested[9] that this negative hollow (diameter ≈ 6 Å) acts as the docking site for positively charged inorganic complexes, which is an attractive possibility. However, broadening of the resonances of Arg42, located very close to the active site and the hollow, Fig. 3, is only observed at the higher concentrations of $[Cr(NH_3)_6]^{3+}$ after the resonances of Tyr82 have already been broadened.[18] We conclude that this region is only important mechanistically at the higher concentrations of $[Cr(NH_3)_6]^{3+}$. Concentrations of $[Cr(NH_3)_6]^{3+}$ used in the blocking experiments are however in the range required.

Further important new information regarding the structure of the active site in the dithionite-reduced cluster has come from recent NMR studies on *S. platensis* and *P. umbilicalis*.[19] These experiments have shown that the extra electron in the reduced

cluster resides on the iron nearest the surface and ligated by cysteines 41 and 46 (Fe_A). Electron transfer to a redox partner in the vicinity of Tyr82 would therefore have to be *via* Fe_B ligated by cysteines 49 and 79. This may not be difficult in view of coupling within the active site,[20] but remains a slightly unusual situation.

Using software developed by Beratan and Onuchic[21,22] we have identified the most favourable electron-transfer pathways in this system. Details of the tunnelling pathway model have been described in detail elsewhere.[23] The tunnelling matrix element can be written as in equation (6).[23] The program searches

$$t_{DA} = \text{prefactor} \prod_{i=1}^{n} \varepsilon_i \qquad (6)$$

for combinations of covalent hydrogen-bond and through-space connections that maximise $\Pi\varepsilon$ between the donor and acceptor sites. Exponential decreases in $\Pi\varepsilon$ with distance are predicted for hydrogen-bond and through-space transfer, whereas the decay for covalent jumps is fixed. A direct through-bond pathway is available from the S atom of Cys79 to the C_γ of Tyr82 and features 13 covalent bonds. Through-bond transfers are predicted[21] to be more efficient in terms of electron transfer than either through-hydrogen-bond or through-space transfers, and the electronic coupling decreases are smaller per bond for covalent links. Consequently, this pathway has a coupling value $\Pi\varepsilon = 1.31 \times 10^{-3}$, where ε is the decay factor for coupling, and on this basis is predicted to be the best pathway.[21] An alternative path is *via* Tyr25. The most favourable route from S(Cys79) is as shown in Fig. 4, and involves a through-space jump of 3.35 Å from the CO of Cys79 to the C_δ of Tyr25. However, the pathway model predicts that a through-space transfer is an 'expensive' route and the coupling decreases exponentially with distance. The latter is reflected in the overall coupling value for the pathway, $\Pi\varepsilon = 1.4 \times 10^{-3}$. This value is further decreased as yet another through-space transfer is needed between the two hydrogen-bonded tyrosine rings of 25 and 82, and is regarded unfavourably therefore.[21] However, these two residues are very highly conserved and some sort of physiological function is therefore implicated. For this reason it is difficult entirely to discount such a route.

The pathway approach provides a realistic framework for considering electron transfer from the Fe_2S_2 centre, and provides an interpretation consistent with both NMR and kinetic observations. Electron transfer from Cys79 to the redox partner located in the hollow region leaves open the question of functionality of the two surface tyrosines and the negative patch. At this time it is probably best to regard the two tyrosines, the negative patch as well as the hollow region as collectively defining a region of surface relevant to electron transfer.

Acknowledgements

We thank the SERC and Johnson Matthey Technology Centre for an SERC/CASE Studentship (to E. L.). We are also grateful to the Molecular Recognition Initiative of SERC for Graphics Facilities and postdoctoral support (to N. P. T.), and to Professor D. A. Beratan and colleagues for information relevant to their program.

References

1 Y. Takahashi, T. Hase, K. Wada and H. Matsubara, *Plant Cell Physiol.*, 1983, **24**, 189.
2 N. Sakihama, M. Shin and H. Toda, *J. Biochem.*, 1986, **100**, 43.
3 H. Matsubara and T. Hase, in *Protein and Nucleic Acids in Plant Systematics*, eds. U. Jensen and D. E. Fairbrothers, Springer, Berlin, 1982, p. 168.
4 F. A. Armstrong and A. G. Sykes, *J. Am. Chem. Soc.*, 1978, **100**, 7710.
5 F. A. Armstrong, R. A. Henderson and A. G. Sykes, *J. Am. Chem. Soc.*, 1979, **101**, 6912.
6 I. K. Adzamli, A. Petrou, A. G. Sykes, K. K. Rao and D. O. Hall, *Biochem. J.*, 1983, **211**, 219.
7 W. R. Rypniewski, D. B. Breiter, M. M. Benning, G. Wesenberg, B.-H. Oh, J. L. Markley, I. Rayment and H. M. Holden, *Biochemistry*, 1991, **30**, 4126.
8 T. Tsukihara, K. Fukuyama, M. Nakamura, Y. Katsube, N. Tanako, M. Kakudo, K. Wada, T. Hase and H. Matsubara, *J. Biochem.*, 1981, **90**, 1763.
9 T. Tsukihara, K. Fukuyama, M. Mizuchima, T. Havioka, M. Kusunoki, Y. Katsube, T. Hase and H. Matsubara, *J. Mol. Biol.*, 1990, **216**, 399.
10 M. T. Borchort and J. S. C. Wessels, *Biochim. Biophys. Acta*, 1970, **197**, 78.
11 M. Plesničar and D. S. Bendall, *Biochim. Biophys. Acta*, 1970, **197**, 192.
12 M. P. Jackman, J. D. Sinclair-Day, M. J. Sisley, A. G. Sykes, L. A. Denys and P. E. Wright, *J. Am. Chem. Soc.*, 1987, **109**, 6443.
13 W. A. Kratz and J. Meyers, *Am. J. Bot.*, 1955, **42**, 282.
14 T.-M. Chan and J. L. Markley, *Biochemistry*, 1983, **22**, 5982.
15 J. Bjerrum and J. P. Reynolds, *Inorg. Synth.*, 1964, **2**, 216.
16 C.-S. Lee, E. M. Gorton, H. M. Neumann and H. R. Hunt, *Inorg. Chem.*, 1966, **5**, 1397.
17 W. M. Latimer, in *Oxidation Potentials*, 2nd edn., Prentice-Hall, Englewood Cliffs, NJ, 1952.
18 T.-M. Chan, E. L. Ulrich and J. L. Markley, *Biochemistry*, 1983, **22**, 6002.
19 L. B. Dugad, G. N. La Mar, L. Banci and I. Bertini, *Biochemistry*, 1990, **29**, 2263.
20 W. H. Orme-Johnson and R. H. Sands, in *Iron Sulfur Proteins*, ed. W. Lovenberg, Academic Press, New York and London, 1973, vol. 2, pp. 195–240.
21 D. N. Beratan and J. N. Onuchic, *Photosynth. Res.*, 1989, **22**, 173.
22 J. N. Betts, D. N. Beratan and J. N. Onuchic, unpublished work.
23 D. N. Beratan, J. N. Onuchic, J. N. Betts, B. E. Bowler and H. B. Gray, *J. Am. Chem. Soc.*, 1990, **112**, 7915.

Received 20*th September* 1991; *Paper* 1/04861I